NeuroImage: Clinical 28 (2020) 102428

Contents lists available at ScienceDirect

NeuroImage: Clinical

journal homepage: www.elsevier.com/locate/ynicl

Quantitative MRI outcomes in child and adolescent leukemia survivors: Evidence for global alterations in gray and white matter

Ellen van der Plas[a], T. Leigh Spencer Noakes[b,c], Darci T. Butcher[d,e], Rosanna Weksberg[d,f,g,h], Laura Galin-Corini[c], Elizabeth A. Wanstall[i,j], Patrick Te[c,k], Laura Hopf[i], Sharon Guger[i], Brenda J. Spiegler[i,l], Johann Hitzler[l,m,n], Russell J. Schachar[o,p], Shinya Ito[c,k,q], Brian J. Nieman[b,c,r,s,*]

[a] Department of Psychiatry, University of Iowa Hospital & Clinics, Iowa City, IA, USA
[b] Mouse Imaging Centre, Hospital for Sick Children, Toronto, ON, Canada
[c] Translational Medicine, Hospital for Sick Children, Toronto, ON, Canada
[d] Genetics & Genome Biology, Hospital for Sick Children Research Institute, Toronto, ON, Canada
[e] Department of Pathology and Molecular Medicine, McMaster University, Hamilton, ON, Canada
[f] Clinical and Metabolic Genetics, Hospital for Sick Children Research Institute, Toronto, ON, Canada
[g] Department of Molecular Genetics, University of Toronto, Toronto, ON, Canada
[h] Institute of Medical Sciences, University of Toronto, Toronto, ON, Canada
[i] Department of Psychology, The Hospital for Sick Children, Toronto, ON, Canada
[j] Department of Psychology, York University, Toronto, ON, Canada
[k] Clinical Pharmacology and Toxicology, Hospital for Sick Children, Toronto, ON, Canada
[l] Department of Pediatrics, Faculty of Medicine, University of Toronto, Toronto, ON, Canada
[m] Developmental and Stem Cell Biology, Hospital for Sick Children, Toronto, ON, Canada
[n] Division of Hematology/Oncology, Hospital for Sick Children, Toronto, ON, Canada
[o] Department of Psychiatry, Hospital for Sick Children, Toronto, ON, Canada
[p] Psychiatry Research, Hospital for Sick Children, Toronto, ON, Canada
[q] Pharmacology and Toxicology, Faculty of Medicine, University of Toronto, Toronto, ON, Canada
[r] Ontario Institute for Cancer Research, Toronto, ON, Canada
[s] Department of Medical Biophysics, University of Toronto, Toronto, ON, Canada

ARTICLE INFO

Keywords:
Acute lymphoblastic leukemia
Late effects
Magnetic resonance imaging
Chemotherapy
Gray matter
White matter

ABSTRACT

Introduction: Cure rates for pediatric acute lymphoblastic leukemia (ALL) have reached an all-time high (> 90%); however, neurocognitive difficulties continue to affect quality of life in at least a subset of survivors. There are relatively few quantitative neuroimaging studies in child and adolescent ALL survivors treated with chemotherapy only. Use of different outcome measures or limited sample sizes restrict our ability to make inferences about patterns of brain development following chemotherapy treatment. In this study, we used magnetic resonance imaging (MRI) to evaluate brain outcomes in ALL survivors, comparing against a group of typically developing, cancer free peers.

Materials and methods: Participants included 71 ALL survivors, on average 8 years after diagnosis and 8–18 years of age, and 83 typically developing controls. Anatomical MRI was performed to evaluate brain structure; diffusion and magnetization transfer MRI were used to examine brain tissue microstructure.

Results: Successful MRI scans were acquired in 67 survivors (94%) and 82 controls (99%). Structurally, ALL survivors exhibited widespread reductions in brain volume, with 6% less white matter and 5% less gray matter than controls ($p = 0.003$ and 0.0006 respectively). Much of the brain appeared affected – 71 of 90 evaluated structures showed smaller volume – with the most notable exception being the occipital lobe, where no

Abbreviations: ALL, Acute lymphoblastic leukemia; MRI, Magnetic resonance imaging; DTI, Diffusion tensor imaging; N-PhenoGENICS, Neurocognitive-phenome, genome, epigenome and nutriome in childhood leukemia survivors; FLAIR, Fluid attenuated inversion recovery; MT, Magnetization transfer; NIH, National Institutes of Health; IQ, Intelligence quotient; ICBM, International consortium for brain mapping; WM, White matter; GM, Gray matter; CSF, Cerebrospinal fluid; INSECT, Intensity normalized stereotaxic environment for the classification of tissue; ANIMAL, Automatic nonlinear image matching and anatomical labeling; FA, Fractional anisotropy; RD, Radial diffusivity; AD, Axial diffusivity; WISC, Wechsler Intelligence Scale for Children; WAIS, Wechsler Adult Intelligence Scale; FDR, False discovery rate; SD, Standard deviation; CI, Confidence interval

* Corresponding author at: Hospital for Sick Children, Centre for Phenogenomics, 25 Orde Street, Toronto, ON M5T 3H7, Canada.
E-mail address: brian.nieman@sickkids.ca (B.J. Nieman).

https://doi.org/10.1016/j.nicl.2020.102428
Received 11 March 2020; Received in revised form 22 August 2020; Accepted 8 September 2020
Available online 15 September 2020

significant differences were observed. Average full-scale IQ in the survivor and control groups were 95 (CI 92–99) and 110 (CI 107–113), respectively. Using data from the NIH Pediatric MRI Data Repository, we evaluated the extent to which elevated IQ in the control group might affect the structural differences observed. We estimated that two thirds of the observed brain differences were attributable to ALL and its treatment. In addition to the structural changes, survivors showed, on average, globally lower white matter fractional anisotropy (-3%) and higher radial diffusivity (+5%) ($p < 10^{-6}$), but no differences in magnetization transfer ratio.
Conclusions: Neuroanatomical alterations in late childhood and adolescent ALL survivors treated with chemotherapy-only protocols are widespread, with white matter being somewhat more affected than gray matter. These MRI results indicate brain development is altered in ALL survivors and highlight the need to examine how these alterations emerge.

1. Introduction

Pediatric acute lymphoblastic leukemia (ALL) is the most common form of childhood cancer. It is typically diagnosed between 2 and 5 years of age (Howlader et al., 2017). Treatment requires a combination of chemotherapy agents administered across phases over 2–3 years. These intensive protocols are remarkably successful: five-year survival rates currently exceed 90% (Howlader et al., 2017). Unfortunately, even with elimination of craniospinal radiation, ALL survivors are at risk of developing cognitive or behavioral problems which may include impairments in processing speed (Jacola et al., 2016; Liu et al., 2018; van der Plas et al., 2018), working memory (Iyer et al., 2015; van der Plas et al., 2018), attention (Krull et al., 2013; Iyer et al., 2015; Jacola et al., 2016; Liu et al., 2018; van der Plas et al., 2018), executive function (Liu et al., 2018) and motor coordination (Iyer et al., 2015; van der Plas et al., 2018).

Several MRI studies in ALL survivors have pointed to the potential role of abnormal brain development or pathology in poor outcomes after treatment. Leukoencephalopathy was reported in ~ 25% of on-treatment ALL patients and was associated with increased risk of long-term behavioral problems (Cheung et al., 2016). Other differences are reported to include smaller total and regional gray and white matter volumes, lower fractional anisotropy (FA), and increased diffusivity (Aukema et al., 2009; Edelmann et al., 2014; Reddick et al., 2014; Krull et al., 2016; van der Plas et al., 2017). Both differences in volume (Reddick et al., 2014; Edelmann et al., 2014; van der Plas et al., 2017) and in diffusion tensor imaging (DTI) measurements (Aukema et al., 2009; Cheung et al., 2016; Darling et al., 2018) have been associated with cognitive outcomes, including executive function (Cheung et al., 2016), processing speed (Aukema et al., 2009; Cheung et al., 2016), working memory (Edelmann et al., 2014; Cheung et al., 2016; van der Plas et al., 2017), as well as intelligence and academic performance (Edelmann et al., 2014; Reddick et al., 2014). However, a recent meta-analysis identified only 10 published neuroimaging studies with control groups that focused on ALL survivors treated with chemotherapy alone (Zhou et al., 2020), 90% of which included < 30 survivors.

The interpretation of brain structure differences in ALL survivors can depend significantly on selection of an appropriate control group. Comparisons to typically developing controls versus to population norms, where available, often result in different findings (Godoy et al., 2020). For studies in children, where ethical and institutional restrictions limit recruitment strategies, it is generally the case that recruited control subjects have an elevated average full-scale IQ. Recent reviews and meta-analyses highlight that this has been true in studies of ALL survivors as well (Iyer et al., 2015; Zhou et al., 2020). The extent to which this influences interpretation of brain structure findings is unclear. As a result, our understanding of the effects of childhood ALL and contemporary chemotherapy treatment on the brain remains incomplete.

The primary aim of the present study was to conduct a systematic evaluation of brain structure in late childhood and adolescent ALL survivors who were treated with contemporary chemotherapy-only protocols. We collected neuroimaging data including MRI scans to evaluate brain structure volumes, as well as regional cortical areas and thicknesses. Our primary objective was to quantify brain structure differences between ALL survivors and typically developing peers. We further used diffusion tensor imaging (DTI) to evaluate microstructural differences in white matter affecting water diffusion. As a secondary aim, we investigated the implications of full-scale IQ in the typically developing control group on our overall findings and evaluated associations between full-scale IQ and brain structure differences in both ALL survivors and typically developing peers.

2. Materials and methods

2.1. Participants

This study was conducted at the Hospital for Sick Children (Toronto, Canada) in conjunction with another study called N-PhenoGENICS that evaluated cognitive abilities, genetic variation and nutrition in ALL survivors (van der Plas et al., 2018). The present study expanded the parent study by adding a typically developing comparison group and neuroimaging. ALL participants were considered eligible if they: (1) were diagnosed with ALL between 1 and 10 years of age; (2) were treated with chemotherapy only (no cranial radiation or bone marrow transplant); (3) completed treatment at least 2 years prior to participation; (4) were able to complete neuroimaging without sedation (as per ethical guidelines prohibiting use of sedation for research purposes only); (5) did not have a diagnosis of Down syndrome; (6) were not currently taking psychoactive medication; (7) did not have a history of head trauma; and (8) were between 8 and 18 years old at evaluation. Participants were drawn from an eligible population of 155 individuals (Fig. 1).

We also recruited typically developing controls (CTL) by posting advertisements on message boards at the Hospital for Sick Children. Interested parents/caregivers contacted team members to establish eligibility by completing screening questions that included items about history of mental health, head trauma, and current psychoactive medications. Participants in the CTL group completed the same neuroimaging protocol as the ALL survivor group. CTL participants were eligible to participate if they had no MRI contraindications, had not been previously diagnosed with a neurodevelopmental disorder, had no history of serious head trauma, were not currently taking psychoactive medication, and were between 8 and 18 years old. Initial recruitment targets for the study were 150 participants in total, split approximately evenly between ALL and CTL groups. Recruitment was adapted over the course of the study to ensure age and sex were comparable between the groups, which resulted in a final total of 71 ALL survivors and 83 CTL participants. Note that a subset of male participants (7 ALL survivors) were included in a previous neuroimaging study that employed identical recruitment strategies as the present study (van der Plas et al., 2017).

General cognitive abilities in all participants in the ALL and CTL groups were assessed using the Wechsler Intelligence Scale for Children IV (WISC) (Wechsler, 2004) for individuals 16 and under and the Wechsler Adult Intelligence Scale IV (WAIS) (Wechsler, 2008) for

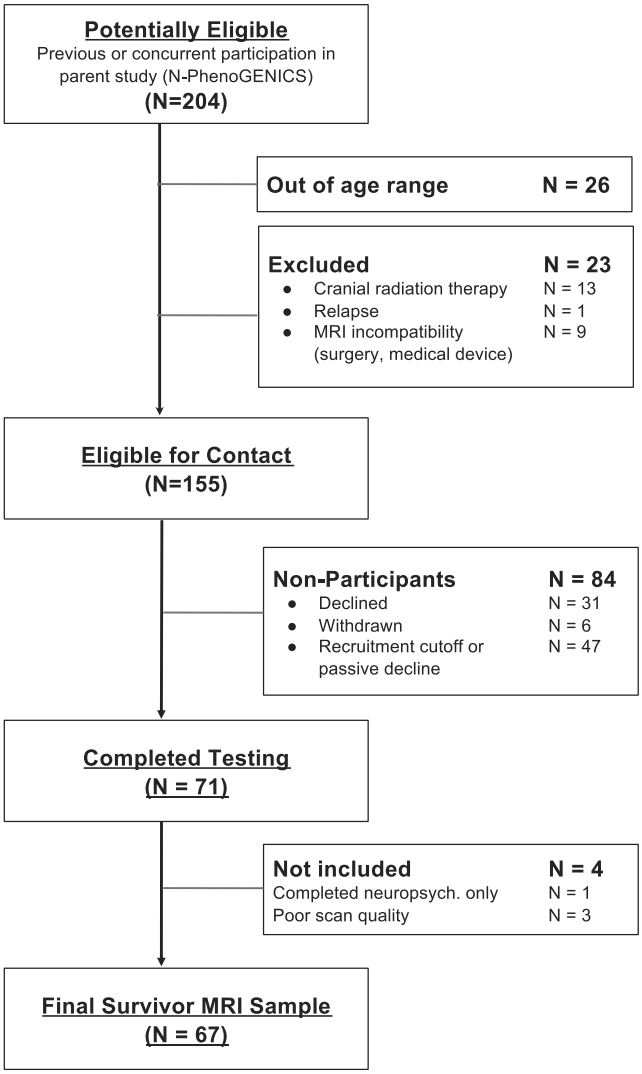

Fig. 1. Consort diagram of ALL participants. Survivors were drawn from a pool of participants in another study (N-PhenoGENICS). A total of 155 were considered eligible for the present study. A total of 150 participants were planned for completion of testing, with approximately half survivors and half controls.

participants who were 17 or older (5 ALL, 6 CTL).

All procedures and study-related communications with participant families were conducted in accordance with a written protocol approved by the Hospital for Sick Children's Research Ethics Board. Informed consent was obtained from all participants, and/or their parents/guardians. Assent was obtained from participants considered unable to provide informed consent.

2.2. Magnetic resonance imaging

Eligible participants were scanned on a 3-Tesla Siemens Trio Tim or Prisma^{fit} MRI system running syngo software. The imaging protocol consisted of the following scans: T_1- and T_2-weighted anatomical scans, a fluid attenuated inversion recovery scan, a diffusion tensor imaging (DTI) series with 60 directions (b = 1000 s/mm^2), and magnetization transfer (MT) scans. Complete scan parameter details are provided in Supplementary Table 1. One ALL participant was unable to complete scanning on the day of testing, and scans from four participants (3 ALL, 1 CTL) were judged unsatisfactory for analysis.

2.3. Repository MRI data

To address the impact of full-scale IQ on the MRI results, additional reference images were obtained from the NIH Pediatric MRI Data Repository provided by the NIH MRI Study of Normal Brain Development (Evans, 2006). Participants for this study were also recruited from the community and were excluded if they had a behavioral disorder, a psychiatric disorder, or a neurological condition. The selected data included 373 images from 175 subjects between the ages of 5 and 21 years old. From these, we generated two subgroups by matching to the recruited CTL and ALL participants: (1) a group matching CTL based on age, sex and full-scale IQ; and (2) a group matching the ALL group based on age and sex, but selected to have an average full-scale IQ of 100, which is the expected population norm (labeled N_100). Comparison of the N_100 to N_CTL groups allowed evaluation of potential impact of CTL group biases and thus aids interpretation of the ALL-to-CTL differences.

To generate the two subgroups from the NIH data, matching was performed based on sex, age and full-scale IQ. A match between subjects i and j was determined by minimization of a Euclidean distance metric derived from normalized subject differences:

$$D_{i,j}^2 = w_{sex}(sex_i \neq sex_j) + w_{IQ}\frac{(IQ_i - IQ_j)^2}{\sigma_{IQ}^2} + w_{AGE}\frac{(AGE_i - AGE_j)^2}{\sigma_{AGE}^2} \quad (1)$$

where σ represents the standard deviation in the indicated variables (IQ and age). The weighting term w_{sex} was set to be very large to ensure sex match, and w_{AGE} was fixed at 1. The w_{IQ} weighting term was set to 2 for the N_CTL sample and to 20 for the N_100 sample, in order to prioritize matching by IQ and to strictly enforce an average full-scale IQ of 100 for the latter. For the N_100 group, the target IQ for each match was selected from a gaussian distribution with mean 100. Repeat matches within or across the N_CTL and N_100 groups were allowed. Too few low full-scale IQ samples were present in the NIH data set to produce a third group matched to the ALL group based on age, sex and full-scale IQ.

2.4. Image processing

To quantify brain structure differences, MR images were processed through the CIVET pipeline (v2.1.0) using the CBRAIN interface (https://mcin-cnim.ca/technology/cbrain/) (Ad-Dab'bagh et al., 2006). Stereotaxic registration of the T_1-weighted MR images used the ICBM152 linear target (Mazziotta et al., 2001), and gray matter (GM), white matter (WM) and cerebrospinal fluid (CSF) were classified using the INSECT algorithm (Zijdenbos et al., 1998; Tohka et al., 2004). Cortical surfaces were extracted (Kim et al., 2005) to estimate thickness (Jones et al., 2000), surface area and volume for the frontal, parietal, temporal and occipital cortices. Gyrification indices were computed for each hemisphere. Segmentations of the ventricles, putamen, brain stem, subthalamic nuclei, fornix, caudate, and frontal, parietal, temporal and occipital lobe WM were generated using ANIMAL (Collins et al., 1999). Additional structural segmentations were achieved using multiple automatically-generated templates (Chakravarty et al., 2013) with predefined atlases for: the thalamus, globus pallidus, and striatum (Chakravarty et al., 2006); the hippocampus (Winterburn et al., 2013); the amygdala (Entis et al., 2012); and WM structures (Mori et al., 2008). In total, 90 individual volumetric measurements, and 16 measurements each of cortical thickness and surface area were extracted. Additionally, to estimate intracranial volume, twenty-one individual segmentations were generated and then multi-atlas segmentation with label fusion was used to produce segmentations for each individual (Wang et al., 2013).

DTI measurements of FA, radial diffusivity (RD), axial diffusivity (AD), and mean diffusivity (MD) were computed using the FMRIB's Diffusion Toolbox (DTIFit) (Behrens et al., 2007) after correction for

distortion based on B_0 maps. Each diffusion measurement was computed voxelwise and then averaged over the WM volume of individual structures identified in the Johns Hopkins atlas (Mori et al., 2008). The MT ratio was computed from the MT on and MT off images and then likewise averaged by structure.

2.5. Statistical analysis

Outcome measures were fit by regression using a linear model. Outcome in the j^{th} subject was modelled as:

$$V_{(j)} = \beta_0 + \beta_{1(j)}^{mri} + \beta_2 \delta age_{dx(j)} + \beta_3 \delta age_{(j)} + \beta_4 sex + \beta_{5(j)}^{grp} + \beta_{6(j)}^{grp} \delta age_{(j)} + \beta_{7(j)}^{grp} sex_{(j)} \quad (2)$$

The *mri*-superscript coefficient was included to account for scanner differences and was referenced to the Prisma^{fit} configuration. The δ preceding the age and age at diagnosis (age_{dx}) terms indicates representation as differences from the group mean for the modeling (12.2 years and 3.8 years, respectively). Sex differences were defined relative to the average by assigning + 0.5 to males and −0.5 to females. All *grp*-superscripts indicate coefficients factored by group, with the contrast matrix defined so that the ALL and N_100 coefficients both represented differences from their control groups (CTL and N_CTL respectively). Where noted, we further added intracranial volume as a covariate. All statistical tests were two-sided. The false discovery rate (FDR) was used to control for multiple comparisons, with q-values reported to establish significance. Where plotted by group, MRI results were adjusted for sex, age and MRI system using the regression results prior to visualization.

3. Results

3.1. Sample

The study sample included 71 ALL survivors (ALL) and 83 typically-developing controls (CTL) . Sample characteristics for both groups are summarized in Table 1. On average, participants were 12.2 years old (SD = 2.8 years, range 8.0–18.1 years). Mean age at ALL diagnosis was 3.8 years (SD = 1.7 years) and an average of 8.1 years (SD = 2.5 years) had elapsed since diagnosis at the time of testing. A majority of the ALL survivors were treated with either the AALL0331 or AALL0232 protocol, for standard and high risk respectively. The AALL0932 and POG9904 (both standard risk) were also used to treat 6 individuals each; a complete tally by protocol is provided in Table 1.

Average full-scale IQ in the ALL and CTL groups were 95.3 and 109.6, respectively (with 95% confidence intervals [CI] of 92.1–98.5 and 106.9–112.7) (Table 1). The ALL group had significantly lower mean full-scale IQ than both the CTL group ($p < 1 \times 10^{-9}$) and the expected population norm of 100 ($p < 0.005$). The CTL group had a higher than expected full-scale IQ compared to the expected population norm ($p < 1 \times 10^{-8}$), but was consistent with the full-scale IQ of the NIH sample (mean 111.8, CI 110.7 – 113.0). The ALL group mean IQ was comparable to a previous report based on the same eligible survivor population (van der Plas et al., 2018), which reported full-scale IQ of 95.9 (CI 93.4 – 98.4) for 130 participants (average 13.1 years old, 60% male).

3.2. Reduced volume in ALL survivors

MRI morphology measurements revealed widespread differences in the ALL group relative to the CTL group. Total brain volume was 5.0% smaller in ALL survivors (Fig. 2, p = 0.0004), with 4.9% (p = 0.0006)

Table 1
Summary of Participant Groups.

Category	CTL	ALL	p	NIH	N_CTL	N_100
Participants	83	71		373	83	71
Sex						
Female	42	32	0.6	190	42	32
Male	41	39		183	41	39
Ethnicity			0.28	*	*	*
European	36	36				
Asian	16	17				
Mixed/Other	31	18				
Age (y, ± SD)	12.5 ± 2.8	11.9 ± 2.8	0.13	12.1 ± 3.6	12.6 ± 2.8	11.8 ± 2.8
8–9	20	27	0.25	69	18	23
10–11	16	15		77	20	18
12–13	19	12		57	14	11
14–15	19	9		58	17	10
16–18	9	8		55	14	9
Handedness			0.59			
R	74	66		327	75	60
L	9	5		47	8	11
Diagnosis Age (y)	-	3.8 ± 1.7	–	-	-	-
≤2	-	23		-	-	-
3	-	26		-	-	-
4	-	8		-	-	-
5	-	6		-	-	-
6	-	3		-	-	-
≥7	-	5		-	-	-
Treatment Protocol			–			
AALL0331	-	37		-	-	-
AALL0232	-	12		-	-	-
AALL0932	-	6		-	-	-
POG9904	-	6		-	-	-
Other	-	10		-	-	-
Mean full-scale IQ (95% CI)	109.6 (106.9–112.7)	95.3 (92.1–98.5)	7×10^{-10}	111.8 (110.7–113.0)	109.9 (107.4–112.6)	100.4 (99.2–101.6)

* Ethnicity was available in too few NIH subjects for comparison.

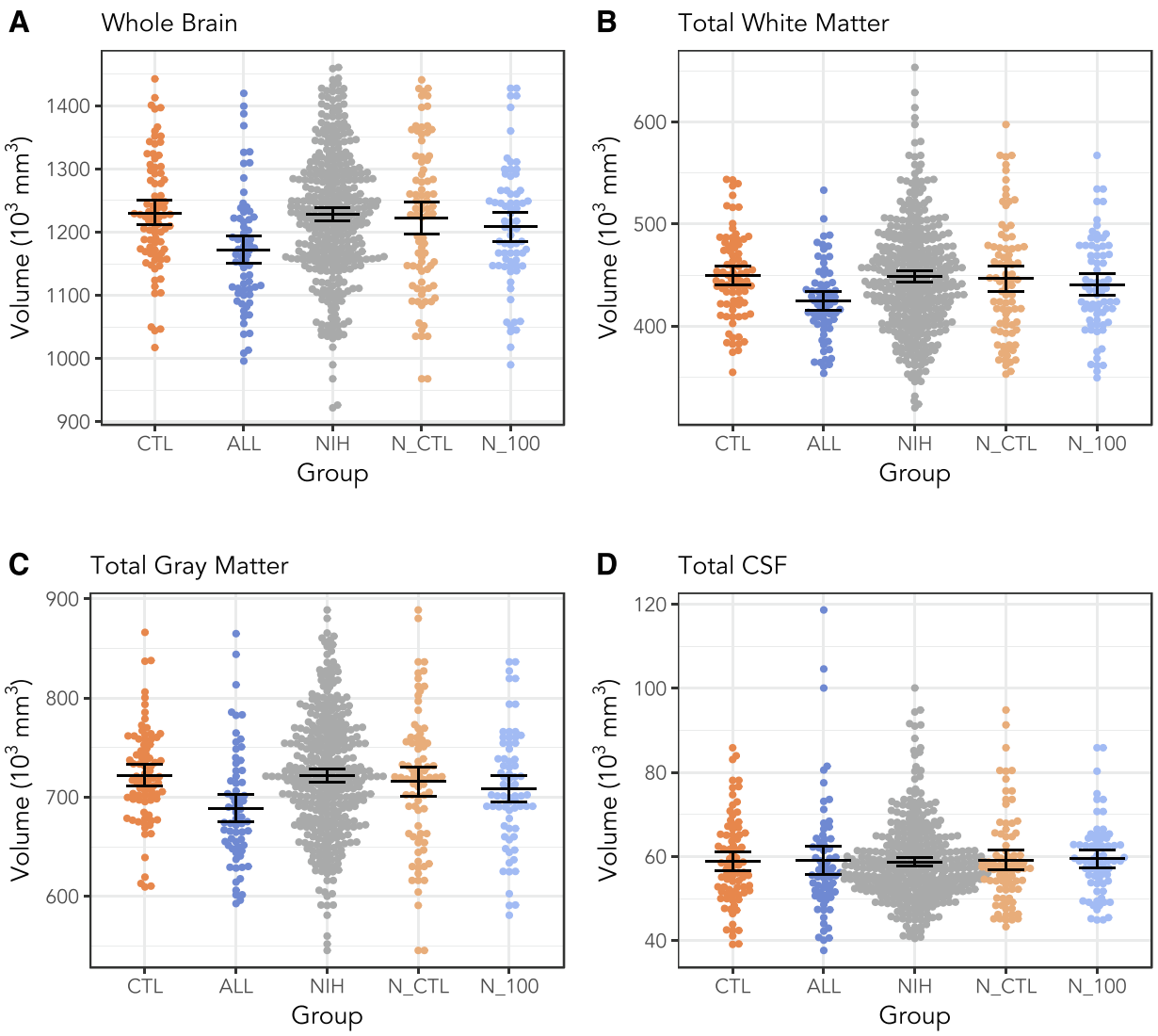

Fig. 2. Comparison of summary volumes in participant groups. Means and 95% confidence limits for volume (y-axis) are shown in black across participant groups (x-axis). The colored circles represent individual observations. Plotted volumes are adjusted for sex and age. ALL survivor participants had significantly smaller total brain (A), total white matter (B) and total gray matter (C) volumes than CTL participants ($p = 0.0004$, 0.003, and 0.0006, respectively). Total cerebrospinal fluid (CSF) volume was not different between groups (D). Three additional groups were formed from the Pediatric MRI Data Repository and are shown as a complete data set (NIH), and matched to the CTL (N_CTL) and ALL groups (N_100, with a target full-scale IQ of 100). No significant differences were noted between the N_100 and N_CTL groups.

and 5.8% ($p = 0.003$) reductions in total gray and white matter volumes respectively. Cerebrospinal fluid (CSF) volumes were comparable between groups. No significant differences were identified in the N_100 group relative to the N_CTL group. Total intracranial volume was 3.8% smaller in ALL survivors compared to CTL (Supplementary Fig. 1, $p = 0.023$). Total brain, gray matter and white matter volume differences between the ALL and CTL groups were still considered significant when covarying for intracranial volume ($p = 0.01$, 0.01, and 0.05, respectively), suggesting relative loss in brain tissue is greater than can be accounted for by smaller intracranial volumes.

Fig. 3 summarizes the regional volumetric differences observed across the brain. Compared with the CTL group, the ALL group had significantly smaller volumes for 71 of the 90 structures evaluated (~80% at $q < 0.1$) (Fig. 3A). Plots for sample individual structures are provided in Fig. 3B-D. Even where not significant, the fitted values uniformly indicated smaller structure volumes in the ALL survivors except in CSF spaces. Supplementary Table 2 shows regression results for all structures. The age term in the linear model was used to estimate age-related volume increase or decrease, providing a cross-sectional estimate of growth rate (e.g., Fig. 3E). The regression estimates indicated a median volume increase of 0.8%/yr over all measured structures in the CTL group. Although we noted that 73% of structures (66 of 90) in the ALL group exhibited reduced age-related volume increase, this difference in slope was not found to be statistically significant in any brain region (Supplementary Table 2).

3.3. Reduced cortical surface area in ALL survivors

Reduced cortical area was observed to be widespread in the ALL survivor group (Fig. 4A). The reduction in surface areas was statistically significant in 11 of the 16 regions evaluated: the frontal lobes (Fig. 4B,C); the temporal lobes; the parietal lobes (D); the parahippocampal cortices; the insula area (bilaterally); and the left cingulate cortex. In contrast, cortical thickness was not significantly different between the ALL and CTL groups, with the exception of a small reduction (2%) in thickness of the isthmus of the left cingulate cortex ($q = 0.01$). We further observed an age-related decrease in cortical thickness (median −0.6%/yr across cortical regions for the

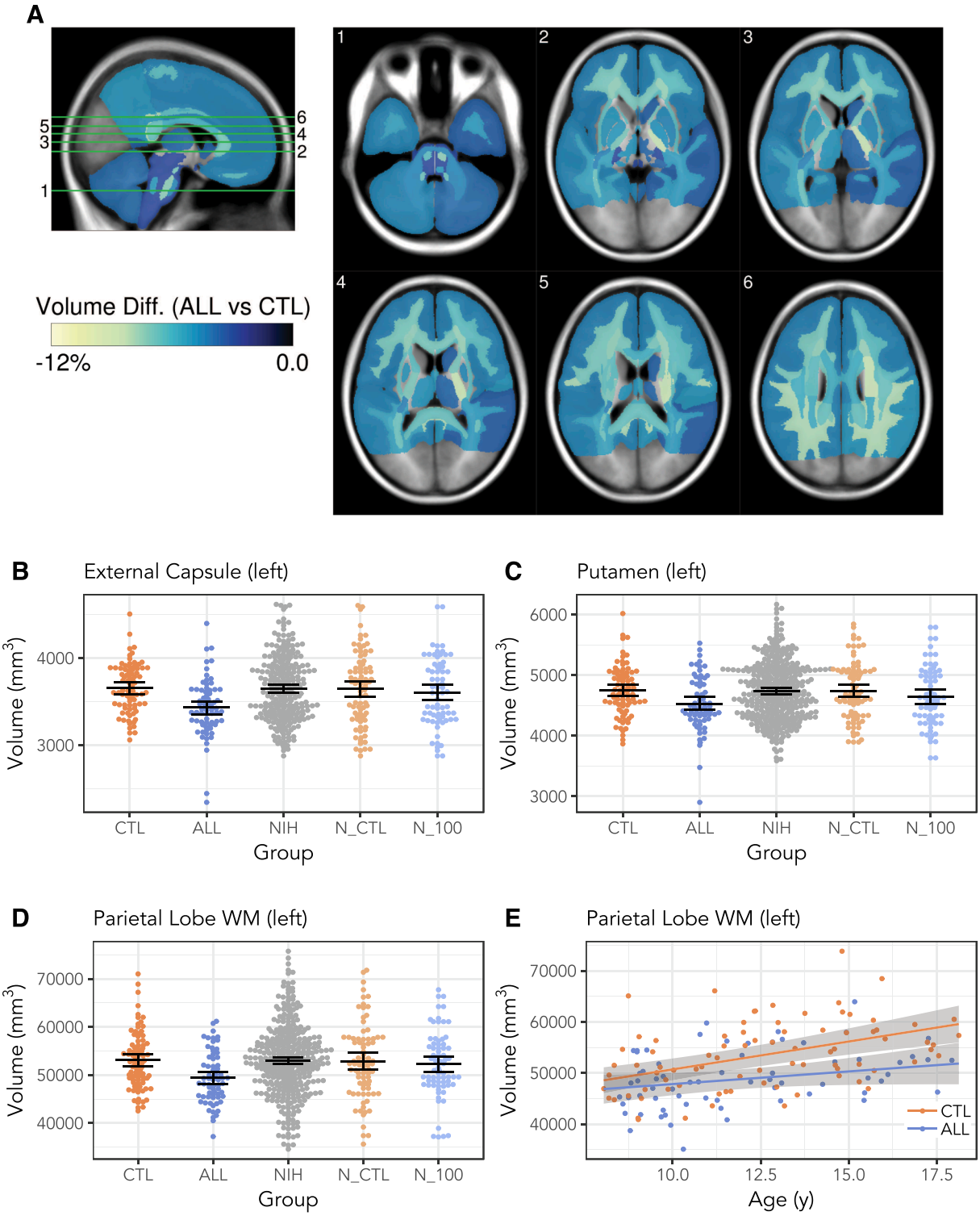

Fig. 3. Volumetric comparisons between ALL survivors (ALL) and typically-developing controls (CTL). In (A), percent volume difference in the ALL group relative to the control is shown mapped to structure for all structures where $q < 0.10$, demonstrating widespread volume differences. Sample plots adjusted for sex and age are shown for the left external capsule (B), putamen (C), and parietal lobe white matter (D). Error bars show 95% confidence intervals about the mean. Cross-sectional evaluation of growth rate was also evaluated. In (E), an example plot of volume (adjusted for sex) versus age is shown for the parietal lobe. The slope was not significantly different ($p = 0.17$).

CTL group). A majority of cortical regions (14 of 16) exhibited a positive age-related increase in cortical thickness for the ALL group relative to the CTL group, possibly suggesting a slowed cortical thinning through development. However, like the age-related volume observations, these trends were not considered significant for any of the cortical regions individually. A sample plot of thickness versus age is provided in Fig. 4E. A complete listing of results by structure is provided in Supplementary Table 2. Gyrification index over the left and right hemispheres were not significantly different (Supplementary Fig. 2).

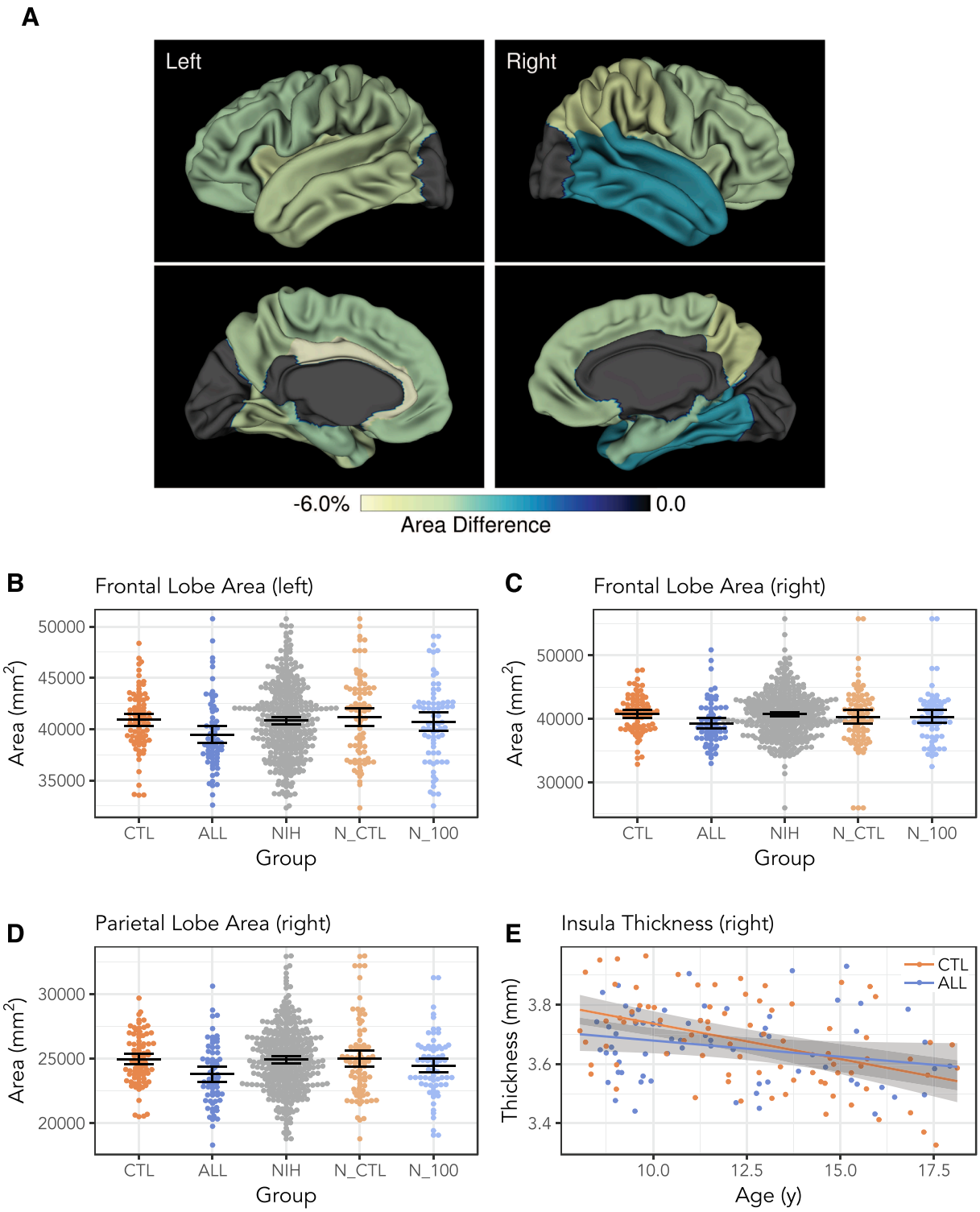

Fig. 4. Cortical area comparisons between ALL survivors (ALL) and typically-developing controls (CTL). In (A), cortical area differences expressed as percent difference in the ALL group relative to the CTL group are mapped across the brain ($q < 0.10$), demonstrating widespread differences. Sample plots of area by group adjusted for sex and age are shown for the left and right frontal lobes (B,C) and for the right parietal lobe (D). Error bars show 95% confidence intervals about the mean. Cross-sectional evaluation of growth rate was also evaluated. In (E), an example plot of cortical thickness (adjusted for sex) versus age is shown for the insula cortex (right). The slope was not significantly different ($p = 0.13$).

3.4. Impact of CTL sample IQ on anatomical findings

We compared neuroanatomy between NIH participants that were matched on sex, age and IQ with the CTL group (N_CTL) and NIH participants that were matched on sex and age to the ALL group with average full-scale IQ of 100 (N_100) (Fig. 5A). No statistical differences were observed between the N_CTL and N_100 groups after FDR correction; however, we did note that 90% of the regression estimates suggested that brain structure volumes tended to be smaller in the N_100 group than in the N_CTL group. To evaluate the possible influence of this bias on our findings, we computed the ratio of the N_100 and ALL regression coefficients for all structures identified as altered in

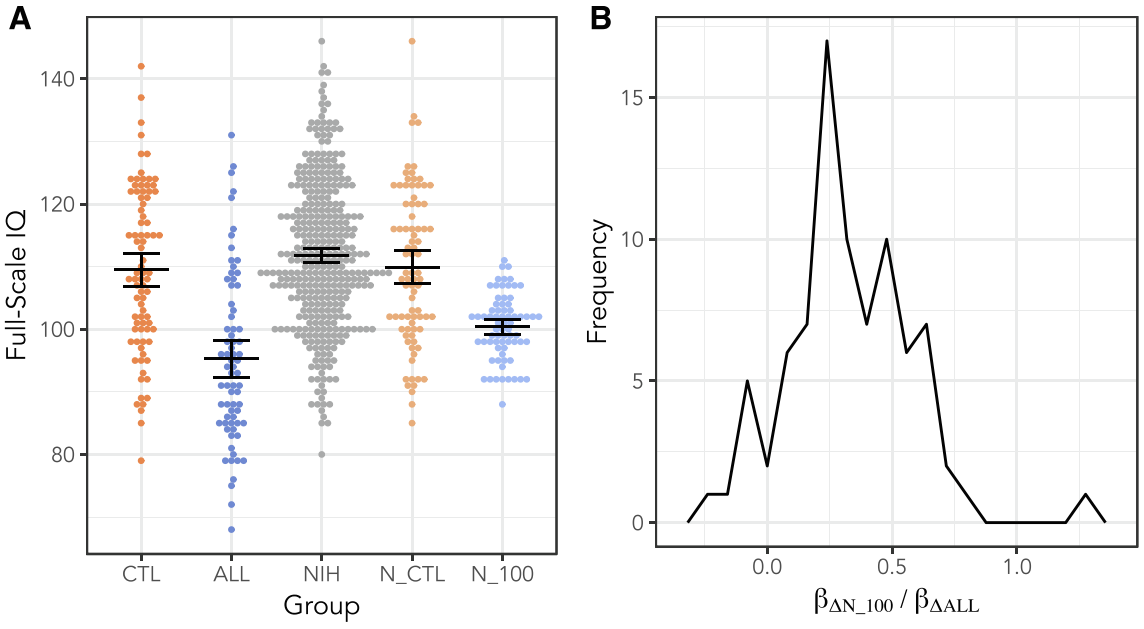

Fig. 5. Comparison of ALL-CTL differences with data from the NIH pediatric MRI data repository. Full-scale IQ is plotted in (A) for the collected ALL and CTL data and all data selected from the pediatric MRI data repository (NIH). Two subgroups drawn from the NIH group: one matched to the CTL group (N_CTL, based on age, sex and full-scale IQ) and the second matched to the ALL group (N_100, based on age and sex, but with an average full-scale IQ of 100). A histogram showing the ratio of the N_100-N_CTL difference to the ALL-CTL difference is shown in (B). All structures that were found to be significantly different in the ALL group were included. The N_100 group showed a similar difference as the ALL group, but averaged only 0.32 times the volume/area difference from N_CTL.

the ALL group (i.e., $\beta_{\Delta N\_100} / \beta_{\Delta ALL}$, where $\beta_{\Delta G}$ is the estimated volume difference between group *G* and its respective control group). A ratio of 0 would indicate that CTL IQ has no effect on neuroanatomical differences between ALL survivors and controls, while a ratio of 1 would indicate that the differences in the ALL group are entirely accounted for by the full-scale IQ of the CTL group. Our analysis yielded an average ratio across structures of 0.32 (0.27–0.37 CI, with std. dev. 0.25), and is depicted as a histogram in Fig. 5B. The ratio, averaged across structures, was significantly different from both 0 and 1 based on a two-tailed *t*-test. We concluded that the elevated IQ of the CTL group likely accounts for about one third of the observed structural reductions in the ALL group based on the N_100-to-N_CTL comparison, but that the balance of the structural differences between groups should be considered specific to the ALL group.

3.5. ALL treatment factors

Since age at diagnosis (von der Weid et al., 2003) and sex (Waber et al., 1992; Brown et al., 1998; Jain et al., 2009) have been identified in previous reports to modulate cognitive outcomes, we tested their association with full-scale IQ and brain structure measurements in the ALL group. Neither were found to be significant in this sample of ALL survivors. We also investigated the possible relationship between full-scale IQ and brain morphology outcomes, after accounting for overall ALL-to-CTL differences. We found no statistically significant associations after correction for multiple comparisons ($q > 0.8$); several plots showing these comparisons are provided in Supplementary Fig. 1 ($p < 0.05$, uncorrected). In addition, treatment protocol was not found to be a significant determinant of either IQ or brain structure outcomes.

3.6. Altered diffusion in ALL survivors

Our primary structure-by-structure analyses revealed no group differences in the DTI and MT data after controlling for FDR. However, a trend did indicate elevated diffusivity in several brain regions (Fig. 6A-F, uncorrected $p < 0.05$). Thus, a secondary analysis was undertaken by comparing the average FA, RD and AD across structures. After averaging across individuals for each structure, a consistent 2.8% decrease in FA and 4.6% increase in RD in the ALL group compared to the CTL group was observed (Fig. 6G-H), suggesting a subtle, global alteration in white matter microstructure in the ALL group compared to the CTL group.

4. Discussion

Our results demonstrate that neuroanatomical abnormalities are widespread in child and adolescent ALL survivors. The largest differences were evident in volume and cortical surface area reductions, which affected most of the brain. Results further indicated lower full-scale IQ in ALL survivors compared to either age-matched controls or population norms. Our structural findings in child and adolescent ALL survivors indicate the presence of brain structure differences following chemotherapy treatment.

Consistent with prior work, our results indicate reduced white matter volume (Zeller et al., 2013; Genschaft et al., 2013; Reddick et al., 2014; Edelmann et al., 2014; van der Plas et al., 2017) and gray matter volume (Zeller et al., 2013; Genschaft et al., 2013; van der Plas et al., 2017) across a broad age spectrum following treatment. We also observed global trends indicating lower FA (-2.8%) linked with higher RD (+4.6%) in ALL survivors, a pattern that has been reported previously (Zou et al., 2017; Darling et al., 2018). The age range of recruited participants (8–18 years of age) allowed us to estimate growth trends in a cross-sectional manner, revealing no significant differences in age-related volumetric or DTI differences between groups. These results suggest that a significant portion of the volume differences observed between groups may occur during or early after treatment, prior to survivor participation in the study.

No significant dependence was observed between ALL clinical history (age at diagnosis, treatment protocol) and brain outcomes. This finding may in part be explained by limited distribution of age at diagnosis in the ALL sample. Targeted recruitment of ALL survivors diagnosed at a later age would likely be needed to elucidate the impact of age at diagnosis. Similarly, treatment protocols are highly standardized, so that true variation in delivered treatment across the participants is

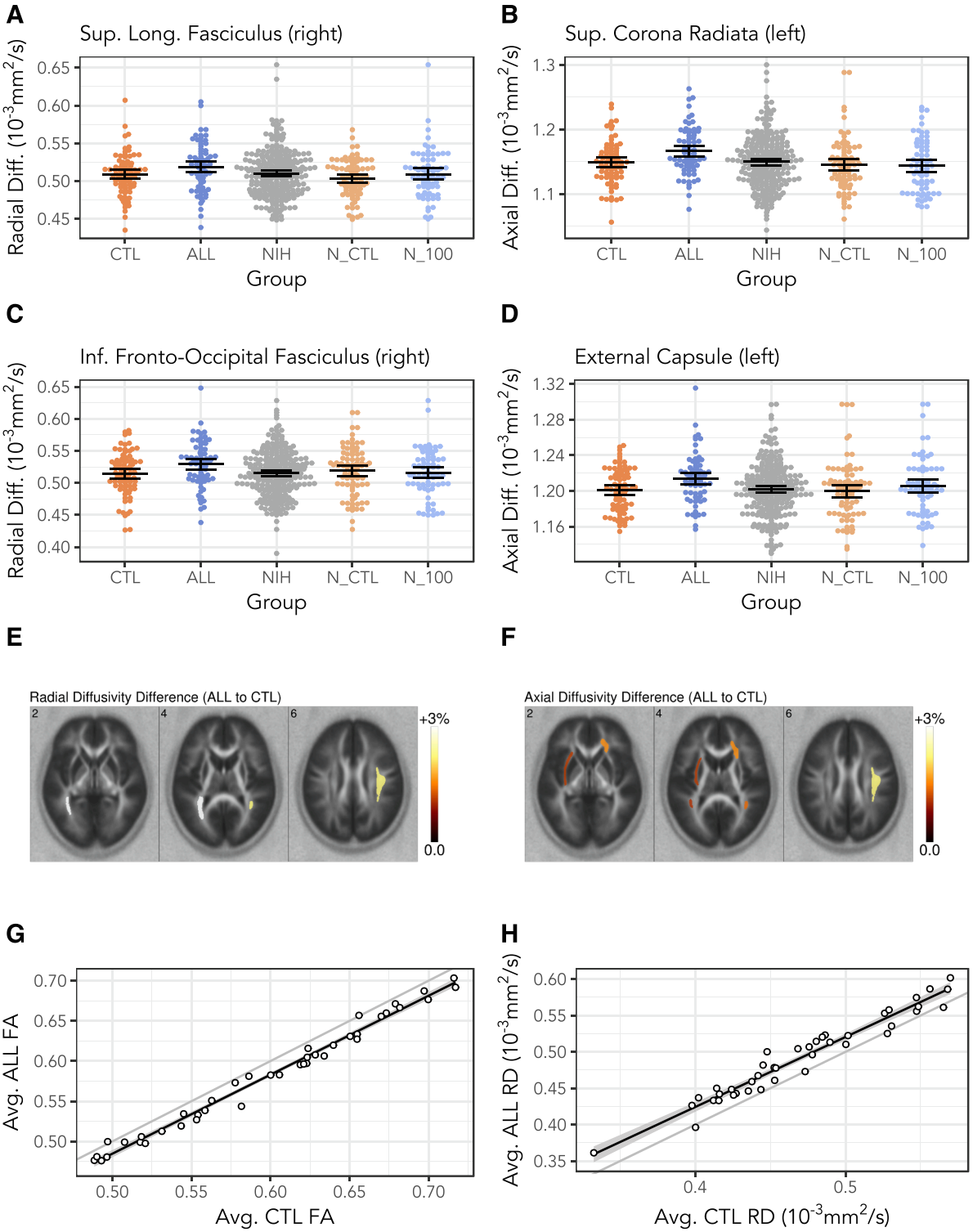

Fig. 6. Comparison of DTI results between ALL and CTL groups. Example radial diffusivities (A, C) and axial diffusivities (B, D) are shown for structures which showed larger deviations in the ALL group. Displayed structures were not significant after correction for multiple comparisons (although uncorrected $p < 0.05$). In (E) and (F), percent difference in ALL compared to CTL in DTI measures are shown for all structures with uncorrected $p < 0.05$ (none were significant after correction for multiple comparisons). Slice numbering matches that in Fig. 3. In (G) and (H), average FA and RD measurements are computed structurewise and plotted with the CTL and ALL averages on the horizontal and vertical axes respectively. A small but widespread decrease in FA and increase in RD is seen across structures. The gray line indicates unity. Black lines indicate best fit with 95% confidence intervals.

likely limited. On the other hand, it is possible that the reported alterations in brain structure in ALL survivors are the result of a mix of factors that encompass clinical history, genetic variation (Kamdar et al., 2011), medical complications (Inaba et al., 2017; Cheung et al., 2018), sociodemographic factors (Peng et al., 2020), as well as their interactions (Cheung et al., 2018). Elucidating the roles of each of these factors is complex. Longitudinal neuroimaging in children undergoing treatment for ALL will be beneficial for studying treatment related factors;

however, this will be a challenging endeavor because young children have difficulty remaining still and treatment-related side effects (nausea, behavioral changes) can further complicate data acquisition. Preclinical models may provide an important alternative approach to investigating these factors and candidate mechanisms. We have already employed this strategy to examine the influence of cranial radiation on brain development (de Guzman et al., 2015, 2019; Beera et al., 2018), including detailed comparisons to human outcomes (Nieman et al., 2015), and for systematic evaluation of ALL chemotherapy agents and their contribution to brain toxicity (Spencer Noakes et al., 2018).

We replicate and extend previous work that identified reduced surface area in ALL survivors (Tamnes et al., 2015). In particular, we found the occipital lobe was conspicuously unaffected in ALL survivors compared to the rest of the cortex (Fig. 4A). More limited growth (Li et al., 2015) and early maturation (Gogtay et al., 2004) in the occipital lobe may make it less sensitive to treatment-related toxicities than other lobes. Another visually striking feature in our findings was an apparent lateralization of ALL surface area differences, with the right temporal lobe less affected than the left (Fig. 4A). Although this visual perception is not statistically significant in the analysis, it may be consistent with reported developmental differences in the left and right temporal lobes (Li et al., 2015). It would be valuable to compare ALL survivors treated at younger versus older ages more broadly to ascertain whether the patterns of structural difference are consistent with developmental stage at diagnosis and treatment. Future work with a larger cohort of ALL survivors diagnosed at later ages (e.g., > 6 y.o.) would be needed to enable this approach.

In line with previous work (Godoy et al., 2020), ALL survivors in the present sample exhibited lower IQ compared with controls. While survivors were not considered clinically impaired compared to population norms, the average full-scale IQ in the ALL survivors (FSIQ = 95.3) was still significantly lower than would be expected for a random sampling of 71 individuals from the normative population. Given the distribution of IQ scores (Fig. 5A), the reduced average may be driven by a small reduction in score across many survivors, rather than a scenario where a few low-scoring individuals drive the group average down. If this is the case, alterations in treatment or post-treatment remediation approaches to improve outcomes may have positive quality of life implications for a majority of survivors.

The present study also provides an important perspective on the potential contributions of full-scale IQ of recruited control participants for studies of brain structure in child and adolescent survivors of childhood cancer. Research studies in ALL survivors, including this one, generally compare against a control group with full-scale IQ higher than expected population norms (Iyer et al., 2015; Zhou et al., 2020). Such group differences could confound the interpretation of brain structural differences between groups, and leaves questions about how much of the reported findings may be artifactual. Utilizing the NIH Pediatric MRI Data Repository, we were able to estimate the relative contribution of elevated IQ (and possibly elevated CTL age, see Table 1) in the control group to the reported structural differences. Approximately one third of the observed overall brain differences were estimated to be attributable to CTL group characteristics (i.e., elevated IQ compared to expected population norms, and age), leaving two thirds of the group differences in brain morphology attributable to factors specific to ALL and its treatment. This result provides confidence that our findings, and those reported previously, are important features of late effect pathology, and not artifactual. Recruitment of typically developing control participants will be an ongoing challenge in the pediatric setting and evaluation of the corresponding impact on interpretation will be important to understanding brain health in ALL survivors.

The co-occurrence of the morphological abnormalities and reduced full-scale IQ in the ALL survivor population naturally leads to speculation about how they might be related. Full-scale IQ generally correlates only poorly with overall brain volume (Pietschnig et al., 2015); however, significant structural abnormalities are expected to affect functional outcomes. Accordingly, several studies have reported brain structure differences in ALL survivors linked with altered cognitive or behavioral scores (Edelmann et al., 2014; Reddick et al., 2014; van der Plas et al., 2017; Darling et al., 2018). After accounting for group (CTL vs ALL), we did not find any such associations between structure measurements and full-scale IQ. Further evaluation of structure as it relates to domain-specific cognitive measures is likely to provide a more meaningful comparison (Hearps et al., 2017).

Some limitations warrant mentioning. The cross-sectional design of the study limited our ability to determine causal relationships between chemotherapy exposures and brain outcomes. We must also consider the possibility of participation bias, both in the CTL and ALL groups, particularly regarding our evidence that full-scale IQ contributes to brain outcomes. While inclusion of the NIH neuroimaging repository mitigated some of this concern, innovative recruitment strategies are required for comprehensive investigation of neurocognitive late effects in ALL survivors (Dixon et al., 2019). Additionally, we found that intracranial volume was significantly reduced in ALL survivors relative to controls. After controlling for ICV, group differences remained significant for only 20% of the regions for which a difference had been detected without ICV as a covariate. Given that ICV is often considered to represent global brain volume attained following development (Edelmann and Krull, 2013; Nopoulos et al., 2011), reductions in ICV may be another manifestation of abnormal development associated with ALL and its treatment. It will be important to determine if certain regions are differentially impacted in ALL survivors.

5. Conclusions

ALL and its treatment have broad and lasting implications for the brain. We demonstrated that ALL survivors exhibit extensive brain structural differences compared to typically developing controls, including volume loss of both gray and white matter, as well as decreased cortical surface area and volume. Determining when these differences in brain structure and function emerge will be an important step in isolating mechanisms of toxicity and designing protective or rehabilitative strategies.

Conflicts of Interest

Dr. R. Schachar has performed consulting work with Ironshore Pharmaceutic and Development, Inc., Purdue Pharma and Lilly Corp. He holds equity in BNAS, a psychological software company and is the Toronto Dominion Bank Chair in Child and Adolescent Psychiatry. The other authors have no conflicts of interest to disclose.

CRediT authorship contribution statement

Ellen van der Plas: Conceptualization, Methodology, Software, Validation, Writing - original draft, Writing - review & editing, Supervision, Funding acquisition. **T. Leigh Spencer Noakes:** Conceptualization, Writing - review & editing. **D.T. Butcher:** Conceptualization, Writing - review & editing. **R. Weksberg:** Conceptualization, Writing - review & editing. **L. Galin-Corini:** Investigation, Data curation. **E.A. Wanstall:** Investigation, Data curation. **P. Te:** Investigation, Data curation, Project administration. **L. Hopf:** Investigation, Data curation, Project administration. **S. Guger:** Conceptualization, Writing - review & editing, Supervision. **B.J. Spiegler:** Conceptualization, Writing - review & editing, Supervision. **J. Hitzler:** Conceptualization, Writing - review & editing, Supervision. **Russell Schachar:** Conceptualization, Writing - review & editing, Supervision. **S. Ito:** Conceptualization, Writing - review & editing, Supervision, Project administration, Funding acquisition. **Brian J. Nieman:** Conceptualization, Methodology, Software, Validation, Formal analysis, Writing - original draft, Writing - review & editing, Supervision, Project administration, Funding acquisition.

Declaration of Competing Interest

The authors declare that they have no known competing financial interests or personal relationships that could have appeared to influence the work reported in this paper.

Acknowledgements

This work was supported by the Ontario Institute for Cancer Research through funding provided by the Government of Ontario (IA-024), the Canadian Institutes of Health Research (142926), and the Canadian Cancer Society (Grant #703558).

Where indicated, reference data used in the preparation of this article were obtained from the Pediatric MRI Data Repository created by the NIH MRI Study of Normal Brain Development. This data was generated through a multi-site, longitudinal study of typically developing children, conducted by the Brain Development Cooperative Group and supported by the National Institute of Child Health and Human Development, the National Institute on Drug Abuse, the National Institute of Mental Health, and the National Institute of Neurological Disorders and Stroke (Contract #s N01-HD02-3343, N01-MH9-0002, and N01-NS-9-2314, -2315, -2316, -2317, -2319 and -2320). A complete listing of the participating sites and investigators can be found at http://www.bic.mni.mcgill.ca/nihpd/info/participating_centers.html. Subject data used for this manuscript can be accessed using Digital Object Identifier 10.15154/1503684 (and at https://nda.nih.gov/study.html?id=669). This manuscript reflects the views of the authors and may not reflect the opinions or views of the NIH. Other data in the manuscript are available from the corresponding author upon request where privacy and ethical restrictions permit.

Appendix A. Supplementary data

Supplementary data to this article can be found online at https://doi.org/10.1016/j.nicl.2020.102428.

References

Ad-Dab'bagh, Y., Einarson, D., Lyttelton, O., Muehlboeck, J.-S., Mok, K., Ivanov, O., Vincent, R.D., Lepage, C., Lerch, J., Fombonne, E., Evans, A.C., 2006. The CIVET Image-Processing Environment: A Fully Automated Comprehensive Pipeline for Anatomical Neuroimaging Research, in: Proceedings of the 12th Annual Meeting of the Organization for Human Brain Mapping. Presented at the Annual Meeting of the Organization for Human Brain Mapping, Florence, Italy.

Aukema, Eline J., Caan, Matthan W.A., Oudhuis, Nienke, Majoie, Charles B.L.M., Vos, Frans M., Reneman, Liesbeth, Last, Bob F., Grootenhuis, Martha A., Schouten-van Meeteren, Antoinette Y.N., 2009. White Matter Fractional Anisotropy Correlates With Speed of Processing and Motor Speed in Young Childhood Cancer Survivors. International Journal of Radiation Oncology*Biology*Physics 74 (3), 837–843. https://doi.org/10.1016/j.ijrobp.2008.08.060.

Behrens, T.E.J., Berg, H. Johansen, Jbabdi, S., Rushworth, M.F.S., Woolrich, M.W., 2007. Probabilistic diffusion tractography with multiple fibre orientations: What can we gain? NeuroImage 34 (1), 144–155. https://doi.org/10.1016/j.neuroimage.2006.09.018.

Brown, Ronald T., Madan-Swain, Avi, Walco, Gary A., Cherrick, Irene, Ievers, Carolyn E., Conte, Paola M., Vega, Roger, Bell, Beverly, Lauer, Stephen J., 1998. Cognitive and Academic Late Effects Among Children Previously Treated for Acute Lymphocytic Leukemia Receiving Chemotherapy as CNS Prophylaxis. J Pediatr Psychol 23 (5), 333–340. https://doi.org/10.1093/jpepsy/23.5.333.

Chakravarty, M. Mallar, Bertrand, Gilles, Hodge, Charles P., Sadikot, Abbas F., Collins, D. Louis, 2006. The creation of a brain atlas for image guided neurosurgery using serial histological data. NeuroImage 30 (2), 359–376. https://doi.org/10.1016/j.neuroimage.2005.09.041.

Chakravarty, M. Mallar, Steadman, Patrick, van Eede, Matthijs C., Calcott, Rebecca D., Gu, Victoria, Shaw, Philip, Raznahan, Armin, Collins, D. Louis, Lerch, Jason P., 2013. Performing label-fusion-based segmentation using multiple automatically generated templates: MAGeT Brain: Label Fusion Segmentation Using Automatically Generated Templates. Hum. Brain Mapp. 34 (10), 2635–2654. https://doi.org/10.1002/hbm.22092.

Cheung, Yin Ting, Sabin, Noah D, Reddick, Wilburn E, Bhojwani, Deepa, Liu, Wei, Brinkman, Tara M, Glass, John O, Hwang, Scott N, Srivastava, Deokumar, Pui, Ching-Hon, Robison, Leslie L, Hudson, Melissa M, Krull, Kevin R, 2016. Leukoencephalopathy and long-term neurobehavioural, neurocognitive, and brain imaging outcomes in survivors of childhood acute lymphoblastic leukaemia treated with chemotherapy: a longitudinal analysis. The Lancet Haematology 3 (10), e456–e466. https://doi.org/10.1016/S2352-3026(16)30110-7.

Darling, Simone J, De Luca, Cinzia, Anderson, Vicki, McCarthy, Maria, Hearps, Stephen, Seal, Marc L, 2018. White Matter Microstructure and Information Processing at the Completion of Chemotherapy-Only Treatment for Pediatric Acute Lymphoblastic Leukemia. Developmental Neuropsychology 43 (5), 385–402. https://doi.org/10.1080/87565641.2018.1473401.

de Guzman, A. Elizabeth, Ahmed, Mashal, Li, Yu-Qing, Wong, C. Shun, Nieman, Brian J., 2019. p53 Loss Mitigates Early Volume Deficits in the Brains of Irradiated Young Mice. International Journal of Radiation Oncology*Biology*Physics 103 (2), 511–520. https://doi.org/10.1016/j.ijrobp.2018.09.014.

Dixon, Stephanie B., Li, Nan, Yasui, Yutaka, Bhatia, Smita, Casillas, Jacqueline N., Gibson, Todd M., Ness, Kirsten K., Porter, Jerlym S., Howell, Rebecca M., Leisenring, Wendy M., Robison, Leslie L., Hudson, Melissa M., Krull, Kevin R., Armstrong, Gregory T., 2019. Racial and ethnic disparities in neurocognitive, emotional, and quality-of-life outcomes in survivors of childhood cancer: A report from the Childhood Cancer Survivor Study. Cancer 125 (20), 3666–3677. https://doi.org/10.1002/cncr.32370.

Edelmann, M.N., Krull, K.R., 2013. Brain volume and cognitive function in adult survivors of childhood acute lymphoblastic leukemia. Transl Pediatr 2, 143–147. https://doi.org/10.3978/j.issn.2224-4336.2013.08.03.

Collins, D.L., Zijdenbos, A.P., Baaré, W.F.C., Evans, A.C., 1999. ANIMAL+INSECT: Improved Cortical Structure Segmentation. In: Kuba, A., Šáamal, M., Todd-Pokropek, A. (Eds.), Information Processing in Medical Imaging. Lecture Notes in Computer Science Springer, Berlin, Heidelberg, pp. 210–223. https://doi.org/10.1007/3-540-48714-X_16.

de Guzman, A.E., Gazdzinski, L.M., Alsop, R.J., Stewart, J.M., Jaffray, D.A., Wong, C.S., Nieman, B.J., 2015. Treatment age, dose and sex determine neuroanatomical outcome in irradiated juvenile mice. Radiat. Res. 183, 541–549. https://doi.org/10.1667/RR13854.1.

Cheung, Y.T., Brinkman, T.M., Li, C., Mzayek, Y., Srivastava, D., Ness, K.K., Patel, S.K., Howell, R.M., Oeffinger, K.C., Robison, L.L., Armstrong, G.T., Krull, K.R., 2018. Chronic Health Conditions and Neurocognitive Function in Aging Survivors of Childhood Cancer: A Report from the Childhood Cancer Survivor Study. J. Natl. Cancer Inst. 110, 411–419. https://doi.org/10.1093/jnci/djx224.

Beera, K.G., Li, Y.-Q., Dazai, J., Stewart, J., Egan, S., Ahmed, M., Wong, C.S., Jaffray, D.A., Nieman, B.J., 2018. Altered brain morphology after focal radiation reveals impact of off-target effects: implications for white matter development and neurogenesis. Neuro-oncology 20, 788–798. https://doi.org/10.1093/neuonc/nox211.

Edelmann, M.N., Krull, K.R., Liu, W., Glass, J.O., Ji, Q., Ogg, R.J., Sabin, N.D., Srivastava, D.K., Robison, L.L., Hudson, M.M., Reddick, W.E., 2014. Diffusion tensor imaging and neurocognition in survivors of childhood acute lymphoblastic leukaemia. Brain 137, 2973–2983. https://doi.org/10.1093/brain/awu230.

Entis, Jonathan J., Doerga, Priya, Barrett, Lisa Feldman, Dickerson, Bradford C., 2012. A reliable protocol for the manual segmentation of the human amygdala and its subregions using ultra-high resolution MRI. NeuroImage 60 (2), 1226–1235. https://doi.org/10.1016/j.neuroimage.2011.12.073.

Evans, Alan C., 2006. The NIH MRI study of normal brain development. NeuroImage 30 (1), 184–202. https://doi.org/10.1016/j.neuroimage.2005.09.068.

Genschaft, M., Huebner, T., Plessow, F., Ikonomidou, V.N., Abolmaali, N., Krone, F., Hoffmann, A., Holfeld, E., Vorwerk, P., Kramm, C., Gruhn, B., Koustenis, E., Hernaiz-Driever, P., Mandal, R., Suttorp, M., Hummel, T., Ikonomidou, C., Kirschbaum, C., Smolka, M.N., 2013. Impact of Chemotherapy for Childhood Leukemia on Brain Morphology and Function. PLoS One 8. https://doi.org/10.1371/journal.pone.0078599.

Godoy, Priscilla Brandi Gomes, Simionato, Natalia Maria, de Mello, Claudia Berlim, Suchecki, Deborah, 2020. Assessment of Executive Functions after Treatment of Childhood Acute Lymphoid Leukemia: a Systematic Review. Neuropsychol Rev 30 (3), 386–406. https://doi.org/10.1007/s11065-020-09446-4.

Gogtay, N., Giedd, J.N., Lusk, L., Hayashi, K.M., Greenstein, D., Vaituzis, A.C., Nugent, T.F., Herman, D.H., Clasen, L.S., Toga, A.W., Rapoport, J.L., Thompson, P.M., 2004. Dynamic mapping of human cortical development during childhood through early adulthood. Proc. Natl. Acad. Sci. 101 (21), 8174–8179. https://doi.org/10.1073/pnas.0402680101.

Hearps, Simone, Seal, Marc, Anderson, Vicki, McCarthy, Maria, Connellan, Madeleine, Downie, Peter, De Luca, Cinzia, 2017. The relationship between cognitive and neuroimaging outcomes in children treated for acute lymphoblastic leukemia with chemotherapy only: A systematic review: Hearps et al. Pediatr Blood Cancer 64 (2), 225–233. https://doi.org/10.1002/pbc.26188.

Howlader, N., Noone, A.M., Krapcho, M., Miller, D., Bishop, K., Kosary, C.L., Yu, M., Ruhl, J., Tatalovich, Z., Mariotto, A., Lewis, D.R., Chen, H.S., Feuer, E.J., Cronin, K.A., 2017. National Cancer Institute SEER cancer statistics review 1975–2014. National Cancer Institute, Bethesda, MD.

Inaba, H., Pei, D., Wolf, J., Howard, S.C., Hayden, R.T., Go, M., Varechtchouk, O., Hahn, T., Buaboonnam, J., Metzger, M.L., Rubnitz, J.E., Ribeiro, R.C., Sandlund, J.T., Jeha, S., Cheng, C., Evans, W.E., Relling, M.V., Pui, C.-H., 2017. Infection-related complications during treatment for childhood acute lymphoblastic leukemia. Ann. Oncol. 28 (2), 386–392. https://doi.org/10.1093/annonc/mdw557.

Iyer, N.S., Balsamo, L.M., Bracken, M.B., Kadan-Lottick, N.S., 2015. Chemotherapy-only treatment effects on long-term neurocognitive functioning in childhood ALL survivors: a review and meta-analysis. Blood 126, 346–353. https://doi.org/10.1182/blood-2015-02-627414.

Jacola, Lisa M., Krull, Kevin R., Pui, Ching-Hon, Pei, Deqing, Cheng, Cheng, Reddick, Wilburn E., Conklin, Heather M., 2016. Longitudinal Assessment of Neurocognitive Outcomes in Survivors of Childhood Acute Lymphoblastic Leukemia Treated on a Contemporary Chemotherapy Protocol. JCO 34 (11), 1239–1247. https://doi.org/10.1200/JCO.2015.64.3205.

Jain, Neelam, Brouwers, Pim, Okcu, M. Fatih, Cirino, Paul T., Krull, Kevin R., 2009. Sex-specific attention problems in long-term survivors of pediatric acute lymphoblastic leukemia. Cancer 115 (18), 4238–4245. https://doi.org/10.1002/cncr.24464.

Jones, S.E., Buchbinder, B.R., Aharon, I., 2000. Three-dimensional mapping of cortical thickness using Laplace's Equation. Hum Brain Mapp 11, 12–32. https://doi.org/10.1002/1097-0193(200009)11:1<12::AID-HBM20>3.0.CO;2-K.

Kamdar, Kala Y., Krull, Kevin R., El-Zein, Randa A., Brouwers, Pim, Potter, Brian S., Harris, Lynnette L., Holm, Suzanne, Dreyer, ZoAnn, Scaglia, Fernando, Etzel, Carol J., Bondy, Melissa, Okcu, M. Fatih, 2011. Folate pathway polymorphisms predict deficits in attention and processing speed after childhood leukemia therapy: Folate SNPs and Neurocognition After ALL. Pediatr. Blood Cancer 57 (3), 454–460. https://doi.org/10.1002/pbc.23162.

Kim, June Sic, Singh, Vivek, Lee, Jun Ki, Lerch, Jason, Ad-Dab'bagh, Yasser, MacDonald, David, Lee, Jong Min, Kim, Sun I., Evans, Alan C., 2005. Automated 3-D extraction and evaluation of the inner and outer cortical surfaces using a Laplacian map and partial volume effect classification. NeuroImage 27 (1), 210–221. https://doi.org/10.1016/j.neuroimage.2005.03.036.

Krull, Kevin R., Brinkman, Tara M., Li, Chenghong, Armstrong, Gregory T., Ness, Kirsten K., Srivastava, Deo Kumar, Gurney, James G., Kimberg, Cara, Krasin, Matthew J., Pui, Ching-Hon, Robison, Leslie L., Hudson, Melissa M., 2013. Neurocognitive Outcomes Decades After Treatment for Childhood Acute Lymphoblastic Leukemia: A Report From the St Jude Lifetime Cohort Study. JCO 31 (35), 4407–4415. https://doi.org/10.1200/JCO.2012.48.2315.

Krull, Kevin R., Cheung, Yin Ting, Liu, Wei, Fellah, Slim, Reddick, Wilburn E., Brinkman, Tara M., Kimberg, Cara, Ogg, Robert, Srivastava, Deokumar, Pui, Ching-Hon, Robison, Leslie L., Hudson, Melissa M., 2016. Chemotherapy Pharmacodynamics and Neuroimaging and Neurocognitive Outcomes in Long-Term Survivors of Childhood Acute Lymphoblastic Leukemia. JCO 34 (22), 2644–2653. https://doi.org/10.1200/JCO.2015.65.4574.

Li, G., Lin, W., Gilmore, J.H., Shen, D., 2015. Spatial Patterns, Longitudinal Development, and Hemispheric Asymmetries of Cortical Thickness in Infants from Birth to 2 Years of Age. J. Neurosci. 35 (24), 9150–9162. https://doi.org/10.1523/JNEUROSCI.4107-14.2015.

Liu, Wei, Cheung, Yin Ting, Conklin, Heather M., Jacola, Lisa M., Srivastava, DeoKumar, Nolan, Vikki G., Zhang, Hongmei, Gurney, James G., Huang, I-Chan, Robison, Leslie L., Pui, Ching-Hon, Hudson, Melissa M., Krull, Kevin R., 2018. Evolution of neurocognitive function in long-term survivors of childhood acute lymphoblastic leukemia treated with chemotherapy only. J Cancer Surviv 12 (3), 398–406. https://doi.org/10.1007/s11764-018-0679-7.

Mazziotta, John, Toga, Arthur, Evans, Alan, Fox, Peter, Lancaster, Jack, Zilles, Karl, Woods, Roger, Paus, Tomas, Simpson, Gregory, Pike, Bruce, Holmes, Colin, Collins, Louis, Thompson, Paul, MacDonald, David, Iacoboni, Marco, Schormann, Thorsten, Amunts, Katrin, Palomero-Gallagher, Nicola, Geyer, Stefan, Parsons, Larry, Narr, Katherine, Kabani, Noor, Goualher, Georges Le, Boomsma, Dorret, Cannon, Tyrone, Kawashima, Ryuta, Mazoyer, Bernard, 2001. A probabilistic atlas and reference system for the human brain: International Consortium for Brain Mapping (ICBM). Phil. Trans. R. Soc. Lond. B 356 (1412), 1293–1322. https://doi.org/10.1098/rstb.2001.0915.

Mori, Susumu, Oishi, Kenichi, Jiang, Hangyi, Jiang, Li, Li, Xin, Akhter, Kazi, Hua, Kegang, Faria, Andreia V., Mahmood, Asif, Woods, Roger, Toga, Arthur W., Pike, G. Bruce, Neto, Pedro Rosa, Evans, Alan, Zhang, Jiangyang, Huang, Hao, Miller, Michael I., van Zijl, Peter, Mazziotta, John, 2008. Stereotaxic white matter atlas based on diffusion tensor imaging in an ICBM template. NeuroImage 40 (2), 570–582. https://doi.org/10.1016/j.neuroimage.2007.12.035.

Nieman, Brian J., de Guzman, A. Elizabeth, Gazdzinski, Lisa M., Lerch, Jason P., Chakravarty, M. Mallar, Pipitone, Jon, Strother, Douglas, Fryer, Chris, Bouffet, Eric, Laughlin, Suzanne, Laperriere, Normand, Riggs, Lily, Skocic, Jovanka, Mabbott, Donald J., 2015. White and Gray Matter Abnormalities After Cranial Radiation in Children and Mice. International Journal of Radiation Oncology*Biology*Physics 93 (4), 882–891. https://doi.org/10.1016/j.ijrobp.2015.07.2293.

Nopoulos, P.C., Aylward, E.H., Ross, C.A., Mills, J.A., Langbehn, D.R., Johnson, H.J., Magnotta, V.A., Pierson, R.K., Beglinger, L.J., Nance, M.A., Barker, R.A., Paulsen, J.S., 2011. Smaller intracranial volume in prodromal Huntington's disease: evidence for abnormal neurodevelopment. Brain 134, 137–142. https://doi.org/10.1093/brain/awq280.

Peng, Liwen, Yam, Perri Pui-Yan, Yang, Lok Sum, Sato, Satomi, Li, Chi Kong, Cheung, Yin Ting, 2020. Neurocognitive impairment in Asian childhood cancer survivors: a systematic review. Cancer Metastasis Rev 39 (1), 27–41. https://doi.org/10.1007/s10555-020-09857-y.

Pietschnig, Jakob, Penke, Lars, Wicherts, Jelte M., Zeiler, Michael, Voracek, Martin, 2015. Meta-analysis of associations between human brain volume and intelligence differences: How strong are they and what do they mean? Neurosci. Biobehav. Rev. 57, 411–432. https://doi.org/10.1016/j.neubiorev.2015.09.017.

Reddick, Wilburn E., Taghipour, Delaram J., Glass, John O., Ashford, Jason, Xiong, Xiaoping, Wu, Shengjie, Bonner, Melanie, Khan, Raja B., Conklin, Heather M., 2014. Prognostic factors that increase the risk for reduced white matter volumes and deficits in attention and learning for survivors of childhood cancers: Reduced WMV in Childhood Cancer Survivors. Pediatr Blood Cancer 61 (6), 1074–1079. https://doi.org/10.1002/pbc.24947.

Spencer Noakes, T. Leigh, Przybycien, Thomas S., Forwell, Amanda, Nicholls, Connor, Zhou, Yu-Qing, Butcher, Darci T., Weksberg, Rosanna, Guger, Sharon L., Spiegler, Brenda J., Schachar, Russell J., Hitzler, Johann, Ito, Shinya, van der Plas, Ellen, Nieman, Brian J., 2018. Brain Development and Heart Function after Systemic Single-Agent Chemotherapy in a Mouse Model of Childhood Leukemia Treatment. Clin Cancer Res 24 (23), 6040–6052. https://doi.org/10.1158/1078-0432.CCR-18-0551.

Tamnes, Christian K., Zeller, Bernward, Amlien, Inge K., Kanellopoulos, Adriani, Andersson, Stein, Due-Tønnessen, Paulina, Ruud, Ellen, Walhovd, Kristine B., Fjell, Anders M., 2015. Cortical surface area and thickness in adult survivors of pediatric acute lymphoblastic leukemia: Cortical Structure in Leukemia Survivors. Pediatr Blood Cancer 62 (6), 1027–1034. https://doi.org/10.1002/pbc.25386.

Tohka, Jussi, Zijdenbos, Alex, Evans, Alan, 2004. Fast and robust parameter estimation for statistical partial volume models in brain MRI. NeuroImage 23 (1), 84–97. https://doi.org/10.1016/j.neuroimage.2004.05.007.

Van Der Plas, Ellen, Erdman, Lauren, Nieman, Brian J., Weksberg, Rosanna, Butcher, Darci T., O'connor, Deborah L., Aufreiter, Susanne, Hitzler, Johann, Guger, Sharon L., Schachar, Russell J., Ito, Shinya, Spiegler, Brenda J., 2018. Characterizing neurocognitive late effects in childhood leukemia survivors using a combination of neuropsychological and cognitive neuroscience measures. Child Neuropsychology 24 (8), 999–1014. https://doi.org/10.1080/09297049.2017.1386170.

van der Plas, Ellen, Schachar, Russell J., Hitzler, Johann, Crosbie, Jennifer, Guger, Sharon L., Spiegler, Brenda J., Ito, Shinya, Nieman, Brian J., 2017. Brain structure, working memory and response inhibition in childhood leukemia survivors. Brain Behav 7 (2), e00621. https://doi.org/10.1002/brb3.2017.7.issue-210.1002/brb3.621.

von der Weid, N, Mosimann, I, Hirt, A, Wacker, P, Nenadov Beck, M, Imbach, P, Caflisch, U, Niggli, F, Feldges, A, Wagner, H.P, 2003. Intellectual outcome in children and adolescents with acute lymphoblastic leukaemia treated with chemotherapy alone: age- and sex-related differences. Eur. J. Cancer 39 (3), 359–365. https://doi.org/10.1016/s0959-8049(02)00260-5.

Waber, D P, Tarbell, N J, Kahn, C M, Gelber, R D, Sallan, S E, 1992. The relationship of sex and treatment modality to neuropsychologic outcome in childhood acute lymphoblastic leukemia. JCO 10 (5), 810–817. https://doi.org/10.1200/JCO.1992.10.5.810.

Wang, H., Suh, J.W., Das, S.R., Pluta, J.B., Craige, C., Yushkevich, P.A., 2013. Multi-Atlas Segmentation with Joint Label Fusion. IEEE Trans. Pattern Anal. Mach. Intell. 35 (3), 611–623. https://doi.org/10.1109/TPAMI.2012.143.

Wechsler, D., 2008. Wechsler adult intelligence scale, 4th ed. Pearson Assessment, San Antonio, TX.

Wechsler, D., 2004. The Wechsler intelligence scale for children, 4th ed. Pearson Assessment, London.

Winterburn, Julie L., Pruessner, Jens C., Chavez, Sofia, Schira, Mark M., Lobaugh, Nancy J., Voineskos, Aristotle N., Chakravarty, M. Mallar, 2013. A novel in vivo atlas of human hippocampal subfields using high-resolution 3T magnetic resonance imaging. NeuroImage 74, 254–265. https://doi.org/10.1016/j.neuroimage.2013.02.003.

Zeller, Bernward, Tamnes, Christian K., Kanellopoulos, Adriani, Amlien, Inge K., Andersson, Stein, Due-Tønnessen, Paulina, Fjell, Anders M., Walhovd, Kristine B., Westlye, Lars T., Ruud, Ellen, 2013. Reduced Neuroanatomic Volumes in Long-Term Survivors of Childhood Acute Lymphoblastic Leukemia. JCO 31 (17), 2078–2085. https://doi.org/10.1200/JCO.2012.47.4031.

Zhou, Chendan, Zhuang, Yong, Lin, Xingjie, Michelson, Alan D., Zhang, Aijun, 2020. Changes in neurocognitive function and central nervous system structure in childhood acute lymphoblastic leukaemia survivors after treatment: a meta-analysis. Br J Haematol 188 (6), 945–961. https://doi.org/10.1111/bjh.16279.

Zijdenbos, Alex P., Jimenez, Alberto, Evans, Alan C., 1998. Pipelines: Large Scale Automatic Analysis of 3D Brain Data Sets. NeuroImage 7 (4), S783. https://doi.org/10.1016/S1053-8119(18)31616-1.

Zou, Liwei, Su, Lianzi, Xu, Jiajia, Xiang, Li, Wang, Longsheng, Zhai, Zhimin, Zheng, Suisheng, 2017. Structural brain alteration in survivors of acute lymphoblastic leukemia with chemotherapy treatment: A voxel-based morphometry and diffusion tensor imaging study. Brain Res. 1658, 68–72. https://doi.org/10.1016/j.brainres.2017.01.017.